Phytoplankton adaptive resilience to climate change collapses in case of extreme events - A modeling study

Boris Sauterey, Guillaume Le Gland, Pedro Cermeño, Olivier Aumont, Marina Lévy, Sergio M Vallina

Phytoplankton adaptive resilience to climate change collapses in case of extreme events – A modeling study

Boris Sauterey[1,3,#], Guillaume Le Gland[2], Pedro Cermeño[2], Olivier Aumont[1], Marina Lévy[1], Sergio M. Vallina[3]

[1]Sorbonne Université, LOCEAN-IPSL, Laboratoire d'Océanographie et du Climat ; Expérimentations et Approches Numériques, Paris, France

[2]Department of Marine Biology and Oceanography, Institute of Marine Sciences (CSIC), Barcelona, Spain

[3]Instituto Español de Oceanografía (CSIC), Gijón, Spain

[#]Corresponding author: boris.sauterey@biologie.ens.fr

Accepted in Ecological Modelling the 06/08/2023

Abstract

As climate change unravels, ecosystems are facing a warming of the climate and an increase in extreme heat events that are unprecedented in recent geological history. We know very little of the ability of oceanic phytoplankton communities, key players in the regulation of Earth's climate by the oceans, to adapt to these changes. Quantifying the resilience of phytoplankton communities to environmental stressors by means of adaptive evolution is however crucial to accurately predict the response of marine ecosystems to climate change. In this work, we use an eco-evolutionary model to simulate the adaptive response of marine phytoplankton to temperature changes in an initially temperate oligotrophic water-column. By exploring a wide range of scenarios of phytoplankton adaptive capacity, we find that phytoplankton can adapt to temperature increases –even very large ones– as long as they occur over the time scale of a century. However, when rapid and extreme events of temperature change are considered, the phytoplankton adaptive capacity breaks down in a number of our scenarios in which primary productivity plummets as a result. This suggests that current Earth System Models implicitly assuming perfect and instantaneous phytoplankton adaptation to temperature might be overestimating the phytoplankton's resilience to climate change.

Introduction

Phytoplankton adaptation and climate change

The photosynthetic release of dioxygen and fixation of carbon and other essential elements (N, P, Fe, Si) by marine microbial communities as they produce biomass is a core component of the biogeochemical machinery regulating the chemistry of the atmosphere and oceans, thereby affecting the climate of our planet (Field et al., 1998; Henson et al., 2011). In turn, the oceanic environment (nutrients availability, temperature, pH, etc.) determines the functioning of phytoplankton communities as phytoplankton acclimates and evolutionarily adapts to the spatial and temporal variability of environmental conditions (Litchman et al., 2012). As climate changes, and will keep changing in the next hundreds of years, phytoplankton will face one of the most rapid and diverse environmental shift in the history of our planet (Bopp et al., 2013), combining global secular trends of ocean warming,

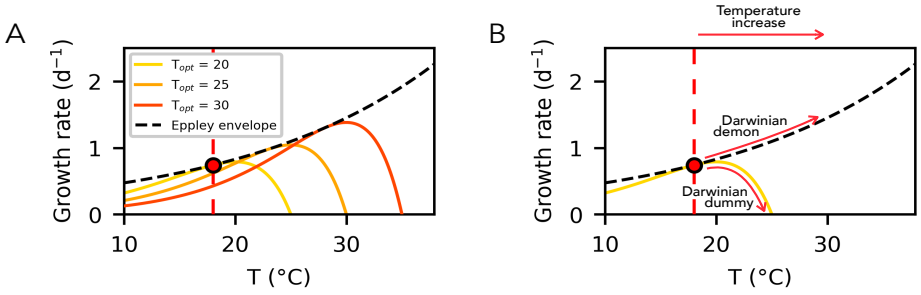

Figure 1: Phytoplankton response to temperature changes. Panel A shows the observed relationship between the growth of phytoplankton individuals and temperature given the thermal niche of those individuals. Each colored thermal reaction norms corresponds to the thermal niche of a specific type of individuals, each niche being characterized by a temperature of optimal growth (T_{opt}). Panel B shows the expected physiological and evolutionary response of phytoplankton communities to a temperature change.

acidification, stratification and desertification to ever more frequent extreme events (e.g., Burger et al., 2022; Gruber et al., 2021). This raises the questions of the ability of marine phytoplankton to evolutionarily adapt to such changes and of the potential implications regarding the continued role of oceans in climate regulation.

The extent of the phytoplankton ability to adapt to environmental changes is currently unknown, but expected to be substantial. Experimental and *in situ* observations (Irwin et al., 2015; O'Donnell et al., 2019; Padfield et al., 2016) tend to suggest that this process can operate in a matter of years. A single liter of oceanic water in the euphotic zone contains 10^6 to 10^9 phytoplankton cells (Flombaum et al., 2013) reproducing approximately once a day (Ward et al., 2017). As the environment changes, the large pool of phytoplankton individuals and their rapid generation time allow advantageous phenotypes either already present or rapidly appearing through mutations (we here use this term in a broad sense to include any mechanisms generating intergenerational phenotypic diversity, e.g., genetic mutations, epigenetic, recombination) to take over communities through selective sweeps. Yet, will adaptive processes be sufficiently rapid to mitigate the potential deleterious effect of climate change on phytoplankton communities? Given how arduous monitoring evolutionary processes in natural systems is and how little we know about the adaptive properties of the phytoplankton as a result, it is for now difficult to answer this question with certainty and to infer how important phytoplankton adaptation to climate change is for the evolution of ocean biogeochemistry. Yet, what we cannot measure *in situ*, we can model *in silico*. As a first step toward answering these questions, we use an ocean model explicitly accounting for the adaptive evolution of the physiological properties of marine phytoplankton under climate change. We explore a wide range of assumptions regarding the adaptive properties of phytoplankton communities and focus specifically on the adaptive response of the phytoplankton to temperature changes.

Phytoplankton and temperature

The response of phytoplankton communities to temperature changes involves two main mechanisms (Eppley, 1972; Grimaud et al., 2017; Norberg, 2004; Fig. 1A and S1). At the scale of individual cells, growth is typically maximized for a given temperature (the optimal growth temperature, T_{opt}), above and below which growth drops to zero, the drop being much swifter towards warmer temperatures (see supplementary discussion). The resulting thermal reaction norm represents the thermal niche of an individual phytoplankton cell or, in other words, the physiological ability of this individual to tolerate (or acclimate to, Grimaud et al., 2017) temperature changes.

Every one of these thermal reaction norms can be placed under an increasing power law envelope. This so-called Eppley envelope (from the pioneering work of Richard Eppley, 1972) thus describes the maximum growth rate achievable by any phytoplankton population given a specific

temperature. Note that here we use the term population to designate a group of phytoplankton individuals having the same value of the trait T_{opt}. In a phytoplankton community composed of several competing phytoplankton populations and in the absence of any other selection pressure, one would expect that the phytoplankton population achieving maximal growth given the temperature of the local environment (i.e., the population whose thermal reaction norm is equal, for the temperature of the system, to the Eppley envelope; Fig. 1A) would outcompete the others in the long run. The Eppley envelope is therefore the optimal evolutionary response of a phytoplankton community to a temperature change (Norberg, 2004). The Eppley envelop is consequently often interpreted as the result of selection operating instantaneously on an infinite standing diversity (perfect species sorting, following Lourens Baas Becking's motto "Everything is everywhere but the environment selects", Baas Becking, 1934). Following Litchman et al., 2012, we define adaptation as natural selection operating on a phenotypically diverse community when the source of diversity is mutation, as is ultimately always the case in biological systems. It follows the Eppley envelop alternatively equivalently corresponds to the result of an instantaneous adaptive process of mutation-selection, i.e., perfect adaptation.

Depending on the assumption made on whether phytoplankton communities can evolutionarily adapt or not to temperature changes, the predicted change in phytoplankton growth in response to a temperature increase therefore switches from one extreme to the other (Fig. 1B). When assuming that phytoplankton communities can adapt perfectly and instantaneously to temperature fluctuations, the growth rate is expected to increase exponentially with temperature. Henceforward, we will call this scenario the Darwinian demon scenario (from Law, 1979). By contrast, when assuming that phytoplankton communities cannot adapt, the phytoplankton response to the temperature change relies solely on its physiology and the growth rate swiftly drops to 0 as temperature increases toward and beyond the tolerance threshold (see supplementary discussion and supplementary table 1). We will call this second scenario the Darwinian dummy scenario.

Which of these two extreme and opposite scenarios is more realistic is expected to depend mostly on the time scale of the temperature change considered. The physiological response of the phytoplankton spans over the lifetime of individuals (few hours to few days, Ward et al. 2017). Evolutionary adaptation on the other hand is a multigenerational process that requires phytoplankton populations carrying newly adapted traits to progressively take over the community, replacing through competitive exclusion older, less adapted populations.

Most global-scale models of marine ecosystems assume that the temperature dependence of phytoplankton growth rate follows an Eppley envelope, regardless of the time scale of the temperature change considered (e.g., Anderson et al., 2021; Henson et al., 2021). In other words and while it is often not interpreted as such (e.g., Henson et al., 2021 state that in their models, phytoplankton "do not evolve or adapt to changing conditions"), those models *de facto* simulate a perfect thermal adaptation by phytoplankton communities.

Is phytoplankton thermal adaptation close to being perfect in natural systems? The relatively good match between the experimentally evaluated thermal norms of phytoplankton populations and *in situ* temperatures (Grimaud et al., 2015; Thomas et al., 2012) constitutes indirect evidence of the ability of phytoplankton communities to adapt to some extent to temperature. This does not provide, however, information on how rapidly adaptation occurs. Monitoring of shifts in the thermal niche of phytoplankton communities *in situ* and in laboratory experiments of artificial selection suggests that adaptation occurs over a few hundreds of generations (one year to a few years depending on the taxa considered; O'Donnell et al., 2019; Padfield et al., 2016). Still, it remains unclear what the actual mechanisms involved in the observed shift in functional composition are; e.g., does it rely on species sorting on a preexisting

standing variation or on selection upon *de novo* diversity generated through mutations (Collins et al., 2014; Litchman et al., 2012)? Furthermore, it is unclear whether general evolutionary properties of phytoplankton communities can be inferred from those observations.

Although few ocean ecosystem models explicitly account for the thermal adaptation of the phytoplankton (but see Demory et al., 2019; Grimaud et al., 2015; Le Gland et al., 2021; Ward et al., 2021; see Ward et al., 2019 for a review of the approaches used to model evolution in ocean ecosystems), none of them addresses the question of the evolutionary response of phytoplankton communities to changing temperatures and of the characteristic time scale of this process. Here we use an eco-evolutionary model explicitly reproducing the functional shift in phytoplankton communities as a result of a mutation-selection process to evaluate the phytoplankton response to long term (secular trend of global warming) and short term (extreme events) temperature changes. We do so in the context of an initially temperate tropical water-column, exploring a wide range of assumptions regarding the adaptive capacity of the phytoplankton in order to address the lack of experimental constraints. The goal is to ask depending on the assumptions of the evolutionary model: How will phytoplankton activity change in response to temperature changes? How reliant on evolutionary adaptation is that change? How wrong are we when we assume perfect and instantaneous adaptation?

Methods

Model

We use the same setup of 1D model of water-column as in Le Gland et al. 2021, which resolves the vertical physics (vertical mixing by turbulent diffusion) of a temperate subtropical system similar to that of the Bermudas (DuRand et al., 2001; Saba et al., 2010). This marine biogeochemical model resolves the dynamics of several plankton populations (phytoplankton and zooplankton) and of the concentration of dissolved and particulate forms of elements (carbon, nitrogen, phosphorous, silicate, iron) essential to phytoplankton growth. Phytoplankton consumes these elements following a Monod formulation (Monod, 1949), and is itself consumed by zooplankton. A recycling term then closes the ecosystem, and the biomass lost to grazing or plankton death is recirculated in the system as dissolved and particulate organic elements (see Le Gland et al., 2021 for details).

The relevance of our model is that, contrary to most ocean ecosystem models, it simulates the variation of the functional composition of the phytoplankton community through time as the result of natural selection. Our approach is based on the SPEAD model (Le Gland et al., 2021; itself adapted from the DARWIN model developed in Follows et al., 2007) that simulates adaptive evolution by means of "trait-diffusion". Instead of simulating the dynamics of a single phytoplankton population with fixed traits as most models do, we simulate the dynamics of the abundance of 50 ecotypes, P_i, each characterized by a specific thermal niche, i.e., by a specific temperature of optimal growth, $T_{opt}(i)$, ranging from 18 to 50.34°C (Fig. 1; both the empirically grounded parametrization of the thermal niche and the range of thermal optima explored are discussed in the supplementary materials). Each of these ecotypes grows and dies depending on the match of its thermal niche to the environmental temperature. At each division event, a mutation can occur so that the produced offspring ends up with a thermal niche different from that of its ancestor (i.e., belongs another ecotypes). This process is driven by a key parameter of the model, ν, which is the probability of mutation per division or mutation rate (see Le Gland et al., 2021; Merico et al., 2014; Smith et al., 2016 and supplementary materials for further details). This parameter determines the ability of the phytoplankton to generate functional diversity through mutation, a necessary condition to Darwinian evolution. Finally, individuals are moved around within the water column through vertical mixing.

To summarize, the functional composition of the phytoplankton community (i.e., the biomass distribution amongst the 50 functional types) varies as the combined result of three explicitly simulated

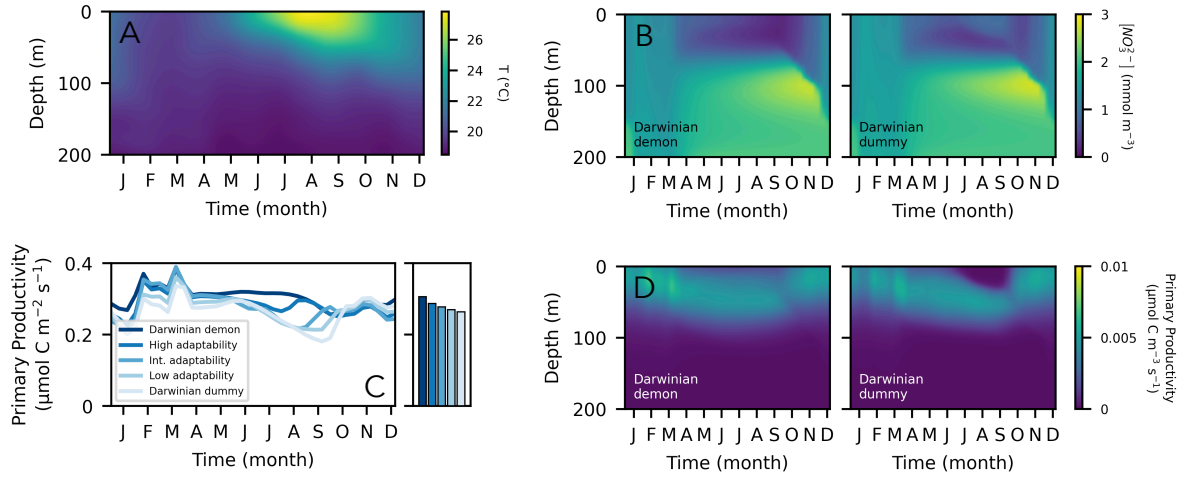

Figure 2: Simulated ecosystem dynamics in the Bermuda-like temperate oligotrophic system. The figure shows the seasonal variation of the vertical profile of the temperature (in °C) (A**)** and of the availability of nitrate (in µmol NO_3^{2-} m^{-3}) (B), and the seasonal variation of the primary productivity (PP) of the phytoplankton (in µmol C m^{-3} s^{-1}) (C and D**)**. The colored curves in panel C correspond to the vertical integration of the predicted PP in five evolutionary scenarios: Darwinian demon, high, intermediate, low mutation rate of the phytoplankton and Darwinian Dummy. The annual means are shown as colorbars on the right hand subpanel. In panels B and D, only the predictions obtained in the two extreme scenarios (i.e., the Darwinian Demon and Dummy scenarios) are shown.

mechanisms : (*i*) mutations, continuously introducing functional diversity in the community; (*ii*) vertical mixing redistributing functional diversity throughout the column; and (*iii*) competitive sorting selecting within the available functional diversity the ecotypes that are the most adapted to the local environmental conditions. The first two mechanisms tend to increase phenotypic diversity in the community. The third mechanism tends to drive it down. Note that our modeling approach typically results in trait distributions being characterized by very long tails, i.e., many non-viable ecotypes are unrealistically maintained in the system at infinitesimal levels by the mutational process. To prevent this from happening, we add an Allee effect (Allee et al., 1949) to our model: below a certain biomass threshold chosen to affect only infinitesimally scarce ecotypes, the biomass specific growth rate of phytoplankton ecotypes steeply decreases with biomass. The main motivation for this strong assumption is therefore to counter an unrealistic feature of continuous population models: their inability to model extinction (see supplementary materials for more discussion and justification).

Finally, note that this type of approach is known to be sensitive to the number of functional types included when this number is too low (Sauterey et al., 2017). We verified that it was not the case by doubling the number of types in the model (100 functional types with thermal optima still ranging from 18 to 50.34°C) in some of our scenarios and obtained quantitatively equivalent results (see the supplementary materials).

Steady state and regimes of climate change

We study the predictions of the model in two types of environmental context. First, we consider the characteristics of the seasonal equilibrium of a temperate oligotrophic system similar to that of the Bermudas. The system alternates between two seasons: a warm and nutrient depleted summer during which the water-column is strongly stratified (from April to October), and a cold and nutrient rich winter during which the stratification of the water column breaks down (from November to March; Fig. 2A and B). Second, we evaluate the changes occurring to the system when it is subject to a regime shift due to climate change, modeled as an increase of the average temperature and/or of the amplitude of the seasonal temperature variation over 100 years. The average temperature increases considered are +2, +4 and +10°C (applied uniformly over the water column), while the amplitude of the seasonal variation in surface

temperatures is increased from 8°C to 18°C. These changes operate linearly over 100 years. Note that in order to artificially isolate the effect of regimes of temperature changes on the ecophysiology of the phytoplankton, the changes in temperature do not feed back onto the physics and chemistry of the water column: nutrient concentrations and the stratification profile of the water-column remain the same as temperature changes, while they would be expected to vary with temperature in an actual water-column. To assess whether such feedbacks could modify our predictions, we evaluated the effect of a drop in nutrient supply due to thermal stratification by decreasing the total nutrient mass in the system in some of the scenarios described above (see Discussion and Supplementary Material).

Evolutionary scenarios

We consider 5 evolutionary scenarios. The first one is the Darwinian demon scenario: there is only one type of phytoplankton, whose growth rate is always maximal (i.e., follows the Eppley envelope) for any given temperature. In other words, the thermal trait T_{opt} of this Darwinian demon is always equal to the evolutionary optimum, noted T^*_{opt}, that maximizes growth given the local temperature (see supplementary materials and Fig. S1B on how we evaluate T^*_{opt}). The second scenario is the Darwinian dummy: there is also only one population of phytoplankton, but its thermal niche is now fixed to make it well adapted to the systems' average surface temperature. Then, in the three remaining scenarios, we run the eco-evolutionary SPEAD model considering a high, an intermediate, and a low value of mutation rate (ν = 10^{-2}, 10^{-5}, 10^{-10}, respectively). In the absence of empirical constraints regarding what phytoplankton mutation rates are in natural systems, those values have been chosen based on preliminary simulations to explore a range as wide as possible. Higher mutation rates become detrimental to phytoplankton mean reproduction rates and adaptive capacity as they result in too many suboptimal types being maintained in the community (Chen et al., 2019; Le Gland et al., 2021). On the other end of the spectrum, lower mutation rates do not allow any diversity to be maintained as mutants are rapidly eliminated by the Allee effect (data not shown). We initialize the simulation with a phytoplankton community composed of a single phytoplankton population characterized by the same thermal niche as the Darwinian dummy in order for the mutational process to be the only source of the emergent functional diversity (the coexistence of multiple ecotypes with different thermal niches) in the phytoplankton community.

Functional composition and maladaptation

At each depth z in the water column, we use the biomass-weighted average optimal growth temperature in the phytoplankton community, $\bar{T}_{opt}(z) = \frac{\sum_i T_{opt}(z) \cdot P_i(z)}{\sum_i P_i(z)}$, as an indicator of the dominant trait in the community. In the Darwinian demon scenario, $\bar{T}_{opt}(z) = T^*_{opt}(z)$, with $T^*_{opt}(z)$ varying in the water-column following the environmental temperature, $T(z)$ (see supplementary materials and Fig. S1B). In the Darwinian dummy scenario, $\bar{T}_{opt}(z)$ always corresponds to prescribed and fixed T_{opt} of the phytoplankton community. The absolute difference between $\bar{T}_{opt}(z)$ and the optimal value of the trait $T^*_{opt}(z)$ of the Darwinian demon (i.e., the value of T_{opt} that maximizes growth given the temperature at z) is then used to evaluate the maladaptation $M(z)$ of the phytoplankton community to its environmental conditions, with $M(z) = \left|\bar{T}_{opt}(z) - T^*_{opt}(z)\right|$. The unit of maladaptation is therefore the °C. Thereafter, we more specifically focus on the average trait and maladaptation of the phytoplankton at the surface ($\bar{T}_{opt}(0)$ and $M(0)$, respectively) where most of the primary productivity (PP) occurs.

Results

Eco-evolutionary response of the phytoplankton to seasonal changes

First, we simulate the seasonal dynamics at equilibrium of our temperate tropical ecosystem in the five scenarios described above: Darwinian demon (perfect and instantaneous adaptation),

Darwinian dummy (no adaptation), and high, intermediate, and low mutation rates.

In the Darwinian demon scenario, biomass production is high during the late winter bloom and drops during the summer (Fig. 2C and D). The water column stratifies during the summer, the nutrient supply to the surface drops, and nutrients in the first 50 meters are depleted by phytoplankton consumption (Fig. 2B). Biomass production during the summer is then limited by the nutrient availability. In the Darwinian dummy scenario, the dynamics of biomass production is similar, except that the drop in productivity during the summer is much more pronounced (Fig. 2C and D). The biomass production in the Darwinian dummy scenario is approximately 15% lower than in the Darwininian demon scenario annually, and up to ~33% lower during the summer. In that case, the dip in production is not the result of a drop in nutrient availability as the nitrate concentration in the mixed layer increases as the summer progresses (Fig. 2B). Instead, it is due to surface temperature surpassing the fixed thermal tolerance of the Darwinian dummy, therefore restricted to deeper regions of the water column (~50 meters) where cooler temperatures prevail throughout the year (Fig. 2A and D). In other words, when the phytoplankton cannot adapt to temperature, the thermal niche of the phytoplankton is, in addition to nutrient availability, a determining factor of biomass production. This confinement of phytoplankton populations to their environmental (thermal) niche is called "environmental filtering" (Vallina et al., 2017). As higher adaptive capacities of the phytoplankton are considered, the phytoplankton is increasingly allowed near the surface, and PP is increasingly high during the summer relative to the Darwinian dummy (Fig. 2C): adaptation, allowing the phytoplankton thermal niche to shift with environmental temperatures, allows it to evade environmental filtering.

When the mutation rate of the phytoplankton is high ($\nu = 10^{-2}$), it adapts "on the fly" to seasonal changes in temperature (Fig. 3A). Near the surface, the distribution of the trait T_{opt} in the community exhibits a single mode. The high mutation rate allows for a rapid succession of events of mutation and selection resulting in a relatively good match between community averaged T_{opt} and the environmental temperature to which it is exposed (Fig. 3D and E). This fast-paced evolution allows a rapid recovery of PP after the initial dip as the summer progresses (Fig. 2C).

When the phytoplankton mutation rate is lower ($\nu = 10^{-5}$ and 10^{-10}) the underlying mechanism to thermal adaptation is fundamentally different as it relies on successive shifts in relative abundance of ecotypes coexisting throughout the year, each being adapted to specific depths and periods of the year (Fig. 3B and C). In other words, the community averaged T_{opt} mostly changes by competitive selection of the most adapted of a pool of pre-existing ecotypes rather than by the selection of new ecotypes appearing through trait mutation. In these scenarios, ecological selection thereby operates on a standing diversity that builds up over the years and is maintained by the spatio-temporal variability of the thermal conditions in the water-column. This result therefore illustrates how the dichotomy between species sorting and adaptation is sometimes artificial given how closely interwoven the standing diversity (on which species sorting applies) and the mutational process (which drives adaptation) are. The lower the mutation rate is, the lower is the extent of the emerging standing diversity (i.e., of the variance of T_{opt} in the community) on which selection can apply, and the higher is the mismatch between the average thermal niche of the phytoplankton and the temperature (Fig. 3D and E). When the phytoplankton mutation rate is the lowest ($\nu = 10^{-10}$), the range of the thermal adaptation becomes so narrow that there is almost no seasonal variability in the community averaged T_{opt}. The phytoplankton community cannot therefore adapt to the warm temperature of the summer, nor to the cold temperature of the winter. The almost constant community averaged T_{opt} corresponds to the annual average of the environmental temperature. As a result, PP throughout the year is very close to that of the Darwinian dummy scenario (Fig. 2C), yet this average "jack of all trades" T_{opt}

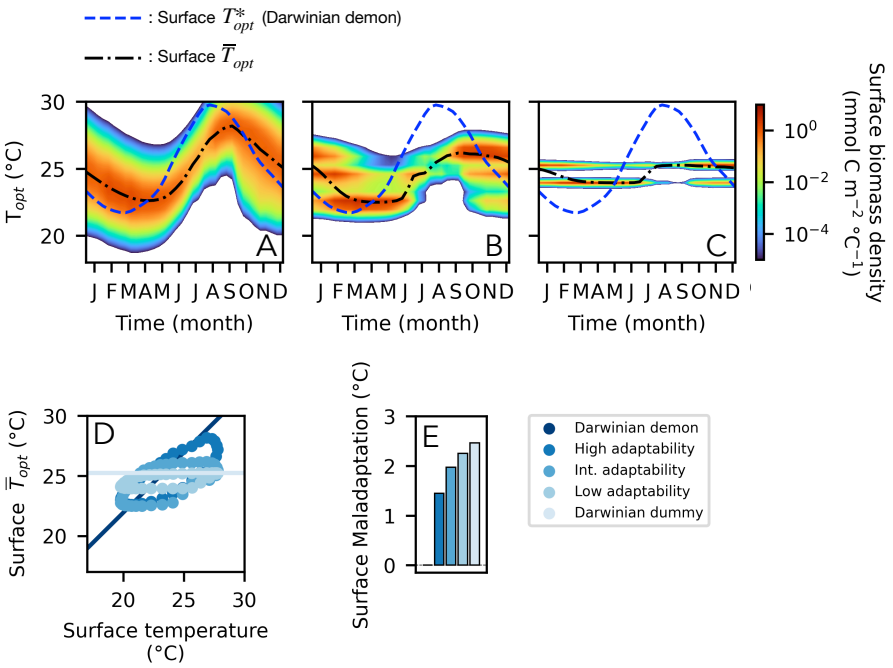

Figure 3: Adaptive response of the phytoplankton to the seasonal change in temperature at the surface. Panels A-C show the seasonal change in the trait distribution of the phytoplankton community in the first meters of the water-column when phytoplankton mutation rate is high, intermediate and low. The black dashed line corresponds to the community average thermal niche at the surface, $\overline{\mathrm{T}}_{\mathrm{opt}}(0)$, and the blue dash-dotted line to the evolutionary optimal trait $\mathrm{T}^*_{\mathrm{opt}}(0)$ (i.e., corresponding to the trait of the perfectly adapting Darwinian demon; see Methods). Panel D shows, the match throughout the year between the average trait of the phytoplankton community at the surface $\overline{\mathrm{T}}_{\mathrm{opt}}(0)$ and the optimal trait $\mathrm{T}^*_{\mathrm{opt}}(0)$ of the Darwinian demon given surface temperatures $\mathrm{T}(0)$ when the phytoplankton has a high, intermediate, and low mutation rate, and when the phytoplankton is a Darwinian dummy (no adaptation). For each of these evolutionary scenarios, the panel E shows the surface thermal maladaptation of the phytoplankton (measured as $\mathrm{M}(0) = \left|\overline{\mathrm{T}}_{\mathrm{opt}}(0) - \mathrm{T}^*_{\mathrm{opt}}(0)\right|$) averaged over the year.

remains the best strategy possible given the limited adaptive capacity of the phytoplankton, allowing phytoplankton to survive the warm and cold extremes of the year.

To sum up, these results highlight that the capacity of the phytoplankton to adapt to seasonal changes in temperature can significantly influence its annual productivity (15% difference in annual PP between perfect and no adaptation), as thermal adaptation promotes the capacity of the phytoplankton to consume nutrients in the mixed layer of the water column throughout the year. Depending on the intensity of the mutational process, adaptation can rely either on a *de novo* diversity produced and selected upon as temperature changes, or on a standing diversity, emerging and maintained over the years. How will phytoplankton productivity change under those various eco-evolutionary regimes in a context of climate change?

Eco-evolutionary response to global climate changes

Climate change is expected to manifest itself both through a secular trend of temperature increase and through more frequent extreme temperature events (Burger et al., 2022; Frölicher et al., 2018; Gruber et al., 2021; Oliver et al., 2019, 2018). To simulate these two phenomena independently and combined, we change the temperature of the water-column by (*i*) imposing a temperature increase without an increase in seasonal amplitude, (*ii*) imposing an increase in seasonal amplitude without changing the average temperature, and (*iii*) imposing simultaneously an increase in average temperatures and in seasonal amplitude (see Methods; Fig. 4A-C). We look at the resulting changes in the annually averaged PP and in the annually averaged community averaged T_{opt} and maladaptation of the phytoplankton community.

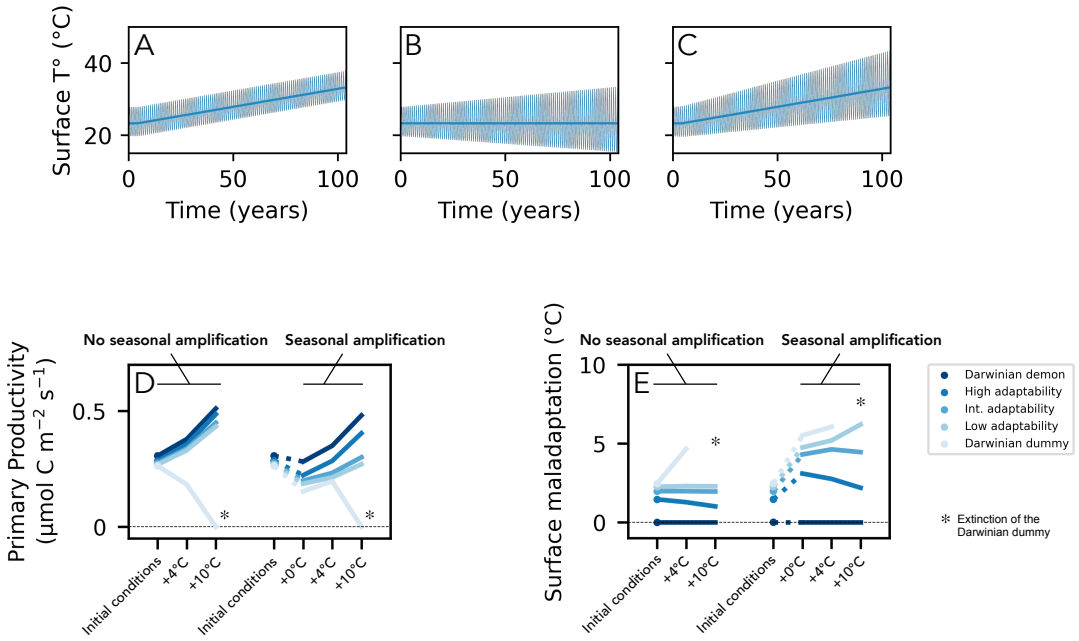

Figure 4: Simulated regimes of temperature change over 100 years (A-C) and phytoplankton primary productivity (D) and surface maladaptation (E) before and after these changes take place depending on the adaptive capacity of the phytoplankton. Climate change is here simulated either as an increase of the average temperatures of up to 10°C (A), as +10°C increase in the amplitude of the seasonal temperature variation (B) or as both simultaneously (C). Panels D and E show the primary productivity and surface maladaptation of the phytoplankton community in the initial conditions of the system and after a global temperature increase of +4 and +10°C coupled or not to an increase in seasonal amplitude. The * signs in panels D and E indicate when there has been an extinction of the phytoplankton population in the Darwinian dummy scenario.

We first consider the consequences of temperature warming up over 100 years without changes in seasonal amplitude. In the Darwinian dummy scenario, PP after 100 years is systematically lower than its initial value, and the phytoplankton community actually collapses when the long-term temperature increase is the strongest (+10°C; Fig. 4D). As the average temperature increases, the phytoplankton community with a fixed (non-adaptive) thermal niche becomes increasingly unfit to near surface environmental conditions (Fig. 4E). During summer, environmental filtering results in phytoplankton being progressively confined to deeper regions of the water column, for longer periods of time. The phytoplankton eventually dies out when the resulting biomass loss becomes too large to be balanced out by biomass production during the winter bloom. By contrast, when phytoplankton individuals are Darwinian demons, a temperature increase results in an increase in PP. The extent of this boost in primary productivity is positively and linearly correla ted to the amplitude of the temperature increase (+11%, +23% and +66% in PP for +2, +4 and +10°C respectively; Fig. 4D). According to the Eppley envelope, the metabolic activity of the phytoplankton accelerates with temperature. As temperature increases and because phytoplankton are able to adapt immediately and perfectly to it, its ability to produce biomass for a given nutrient influx increases (but see the Discussion section). Note that in line with previous work (Archibald et al., 2022), biomass counter-intuitively decreases as PP increases (see supplementary figure 4). Similarly to Archibald et al. (2022), we interpret this dual pattern as an acceleration of the biomass turnover (faster transfer to zooplankton then remineralization). When explicitly including adaptive evolution of phytoplankton in the model, the predicted changes in biomass and PP are very similar despite the large differences in the assumed mutation rates (Fig. 4D). As long as the mutational process is sufficient to sustain some degree of functional diversity, thermal adaptation can proceed. It would therefore appear that the Darwinian demon assumption is a robust approximation of the adaptive capacity of phytoplankton communities. In other words, thermal adaptation is very likely to be sufficiently rapid to keep up with global warming, even for a temperature increase as large as +10°C

over 100 years. In fact, maladaptation remains constant over time at the surface in most scenarios and even drops when the mutation rate is high (Fig. 4E). This latter observation stems from the fact that phytoplankton individuals divide faster as temperature increases, generating more mutants, and the phytoplankton community is able to adapt faster to seasonal changes as a result. This is particularly true when thermal adaptation mostly relies on *de novo* diversity such as in the high mutation rate scenario (Fig. 3A).

We then consider the effect of seasonal amplification with no change in the annually averaged temperature (+0°C in the "seasonal amplification" case in Fig. 4). We observe that PP drops in every evolutionary scenarios, from -8% in the Darwinian demon scenario to -42% in the Darwinian dummy scenario (the other scenarios fall between these two extreme cases; Fig. 4D). The increased seasonality implies colder temperatures during the winter and warmer temperatures during the summer. As temperatures prevailing during the winter bloom get colder (Fig. 4A-C), the phytoplankton metabolism slows down (Fig. 1) and productivity lowers accordingly. This explains the productivity drop in the Darwinian demon scenario in spite of adaptation being perfect (Fig. 4D). Additionally, when adaptation is imperfect, the phytoplankton community progressively becomes unable to adapt to the increasingly large seasonal variation in temperature. This increased maladaptation drives productivity down (-22%, -28% and -31% for high, intermediate and low mutation rates respectively; Fig. 5B). Therefore, contrary to the previous case, the model predicts that mutation rate is a key parameter when increasing the seasonal amplitude without changing the average temperature (Fig. 4D).

To summarize, PP increases with average temperature (except in the Darwinian dummy scenario) but decreases with amplified seasonality. When increasing temperatures and seasonality simultaneously in the Darwinian demon scenario, the negative effect of the seasonal amplification on PP is largely marginal compared to the positive effect of the average temperature increase (+3%, +14% and +57% for +2, +4 and +10°C respectively; Fig. 4D). However, this is not necessarily the case when adaptation is imperfect. The positive effect of a +10°C warming balances out the negative effect of seasonal amplification and leads to PP increasing by 41% when the mutation rate is high, by 8% when it is intermediate, and by 0.2% when the mutation rate is low (Fig. 4E; the phytoplankton still goes to extinction in the Darwinian dummy scenario). However, for a +4°C warming, the negative effect of seasonal amplification dominates and PP drops down (-0.8%, -15% and -20% for high, intermediate and low mutation rates; Fig. 4E).

Overall, we find that primary productivity is expected to increase as global temperatures rise up in the context of a regime of climate change as long as phytoplankton communities are characterized by some capacity to adapt to temperature changes (Fig. 4D and 5). This effect could nevertheless be mitigated by an increase in thermal maladaptation (Fig. 4D-E and 5). Thermal maladaptation is expected to increase as short-term variations of temperature become larger and faster (Fig. 5). The extent of this increased maladaptation then depends on the adaptive capacity of phytoplankton communities determined by their characteristic mutation rate (Fig. 4E). The predictions of our model are therefore especially sensitive to the adaptive capacity of the phytoplankton when increased seasonality is considered (Fig. 4D). As a result, our model predicts anything from a -31% to a +69% change in primary productivity depending on the assumed nature and amplitude of global warming, change in temperature seasonality, and extent of the phytoplankton adaptive capacity (Fig. 4D and 5).

Discussion

Using a 1D ocean model, we simulated the eco-evolutionary response of a phytoplankton community to long term and short-term temperature changes, exploring a wide range of scenarios regarding the evolutionary properties of the phytoplankton –from perfect adaptation to no adaptation at all– and the regime of temperature

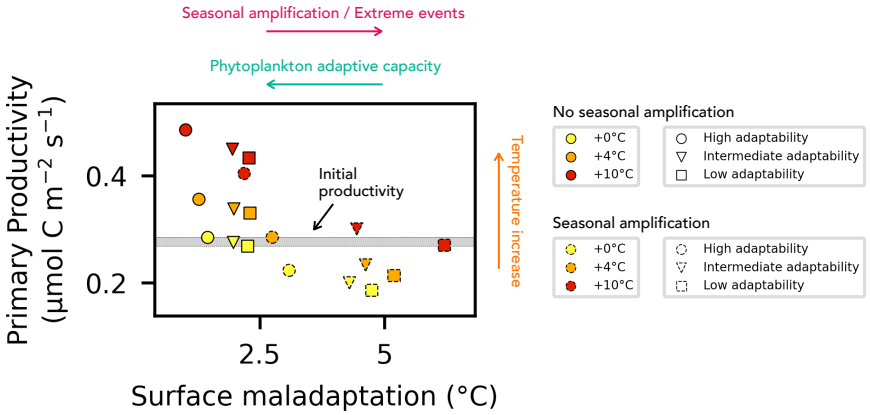

Figure 5: Link between primary productivity, temperature increase and maladaptation of the phytoplankton. Each dot corresponds to the state of the system after 100 years of a temperature increase of +0, +4 and +10°C coupled or not with seasonal amplification. The shape of the dots corresponds to the adaptive capacity of the phytoplankton and their color to the amplitude of the temperature increase over 100 years. Dots corresponding to scenarios of seasonal amplification have dashed edges, those that do not have plain edges. We plotted only the scenarios in which the adaptive capacity of the phytoplankton is high, intermediate and low and excluded the Darwinian demon and dummy scenarios. The arrows correspond to the direction of main effect of seasonal amplification, phytoplankton adaptive capacity, and average temperature increase (in magenta, turquoise and orange respectively) on PP either directly (temperature increase) or indirectly through their effect on maladaptation (seasonal amplification and phytoplankton adaptive capacity).

changes. We found that when climate change is considered solely as a long-term trend of temperature increase, the adaptive response of phytoplankton is in most cases sufficiently rapid for phytoplankton to persist and even to see its biomass production increase, including for very large temperature increases (e.g, 10°C over 100 years; Fig. 4A). The commonly used Darwinian demon approximation then emerges as an acceptable representation of the adaptive capacity of the phytoplankton. However, when the amplitude of the seasonal variability of temperatures increases with the average temperatures, which is likely to occur in a regime of climate change (Frölicher et al., 2018; Gruber et al., 2021; Oliver et al., 2019, 2018), the Darwinian demon approximation is no longer valid. We find that the efficacy of phytoplankton adaptation to increasingly extreme short-term temperature changes is indeed very dependent on the assumed phytoplankton mutation rate. The resulting maladaptation can substantially mitigate the prediction of increased biomass production. In some cases, when the amplitude of those short-term events is large compared to that of the long-term temperature increase, biomass production actually drops down as climate changes (Fig. 5). As primary production is one of the main driving forces of ocean biogeochemistry, our study highlights the importance of phytoplankton adaptation for the resilience of marine ecosystems to climate change. Our results are however obtained in an idealized framework, isolating the response of a local phytoplankton community to temperature changes alone. Several components of climate change and of the phytoplankton's response to it are therefore neglected.

First, adaptation in the ocean is not a purely local process: when traits are locally selected, they can then be exported elsewhere through oceanic circulation and influence –positively or not– the phytoplankton adaptive response across the ocean (Leibold and Norberg, 2004; Loeuille and Leibold, 2008; Sauterey et al., 2017). Similarly, climate change will not just affect temperatures, but a multitude of other characteristics of oceanic systems (nutrient availability, pH, water stratification, horizontal circulation…) over "long" time scales (i.e., the century) but also through extreme compound events (Burger et al., 2022; Gruber et al., 2021). We chose to evaluate in isolation the effect of temperature on the evolution of thermal niches and ignored those additional environmental stresses for simplicity. However, in natural systems under climate change, these

environmental stresses could affect phytoplankton growth and adaptive capacity (Brennan et al., 2017). For instance, climate change is expected to enhance thermal stratification which should lead to a decreased nutrient supply to the euphotic zone, especially during summer. Climate change is also expected to increase depth of the mixed layer and the frequency and intensity of storms, which both tend to increase nutrient supplies by vertical turbulence (Sallée et al., 2021). Predicting how nutrient limitation will evolve under climate change is therefore challenging. Moreover, predicting the combined effect of nutrient limitations and temperature changes on phytoplankton growth and on the capacity of phytoplankton to adapt is a non-trivial issue. Empirical evidence suggests for instance that the effect of temperature changes on phytoplankton growth could be largely nullified in nutrient depleted conditions (Marañón et al., 2018). Although those questions are beyond the scope of this study, we provide some back-of-the-envelope estimates and additional discussion of how changes in nutrient supply affect our results (see Supplementary Material). Although the predicted increase in PP can be reversed by a concomitant decrease in nutrient supply, the main results regarding the sensitivity of PP evolution to the phytoplankton adaptive capacity are qualitatively unaffected. Those additional simulations actually show that the capacity of phytoplankton to adapt to temperature changes is diminished under more nutrient-limited conditions (see supplementary discussion). This suggests that such interacting effects between multiple environmental stressors might play a key role in determining the efficacy of phytoplankton adaptation across oceans (e.g., in nutrient depleted vs nutrient rich regions) and illustrates the need for further investigations. To explore these questions, we plan moving forward to implement our approach in a 3D model of ocean circulation. Such an integrated approach will allow evaluating in a spatially accurate environmental context how dispersal, the spatial distribution of environmental stressors and their covariance across oceans affect phytoplankton adaptation, and how this is expected to change in the context of climate change.

Additionally, several functional traits of phytoplankton communities are expected to evolve simultaneously in response to the combined selective pressures resulting from climate change (e.g., cell-size, traits related to nutrient, pH or light stresses). This raises an intriguing question: how does the simultaneous evolution of multiple traits influence the evolution of each singular trait (see Boyd et al., 2018 and Brennan et al., 2017 for some empirically grounded elements of response and Savage et al., 2007 for a first attempt at modeling multiple traits evolution in phytoplankton)? Similarly, phytoplankton are not the only marine organisms that climate change will affect. Higher trophic levels, characterized by a slower demography hence by a slower pace of evolutionary response will also be impacted by it. The same goes for the recycling microbial loop that determines how much of the organic matter circulating into marine ecosystems is recycled toward the ocean surface and how much is exported to the deep ocean (Cherabier and Ferrière, 2022). Extending our approach to simulate the simultaneous evolution of multiple traits (as done in Le Gland et al., 2021) and the adaptive evolution of populations other than phytoplankton would provide an ideal modeling framework to address those currently unresolved issues.

Finally, as our results suggest that the adaptive capacity of phytoplankton might be a determining factor of the resilience of marine ecosystems to climate change while our very limited quantitative knowledge of what that capacity actually is still remains, we argue that quantitative assessments of phytoplankton adaptive properties becomes an urgent matter. Although experimental work in laboratory remains a viable option, we argue that combining global oceans models including phytoplankton evolution with observational data might constitute a complementary and promising avenue of research. Many macro-scale phenomena such as the emergence of the global biogeography of the thermal niches of the phytoplankton or the response of the phytoplankton to rapid climatic events such as El Niño/La Niña most likely involve, to some extent,

thermal adaptation by the phytoplankton. Ocean-wide meta-genomic data sets (e.g., Chaffron et al., 2021; Sunagawa et al., 2020) and satellite observations (Mouw et al., 2019) are now becoming increasingly available and can be used to infer marine ecosystems' composition and function in such macro-scale contexts. We argue that constraining the parametrization of evolutionary approaches such as ours integrated in 3D models of ocean circulation based on the ability of these coupled models to reproduce those observed global scale phenomena will constitute an efficient way to quantify the adaptive properties of marine ecosystems.

Concluding remarks

Our findings suggest that the resilience of marine ecosystems to climate change, and more specifically to the multiplication of extreme climatic events, will be determined by the ability of phytoplankton communities to adapt. Current Earth System Models implicitly assume that phytoplankton communities are perfectly adapted to their thermal environment at any time and are therefore likely to overestimate marine ecosystems' resilience. While the present exploratory work shows how our limited quantitative knowledge of phytoplankton adaptive properties limits our ability to predict the resilience of marine ecosystems to climate change, it also paves the way toward improving that knowledge through the use of models of phytoplankton evolution. Ultimately, we think that approaches such as ours may play a key role in increasing the accuracy of Earth System Models' climate projections.

References

Allee, W., Park, O., Emerson, A., Park, T., Schmidt, K., 1949. Principles of animal ecology.

Anderson, S., Barton, A., Clayton, S., Dutkiewicz, S., Rynearson, T., 2021. Marine phytoplankton functional types exhibit diverse responses to thermal change. Nature Communications 12, 1–9. https://doi.org/10.1038/s41467-021-26651-8

Archibald, K.M., Dutkiewicz, S., Laufkötter, C., Moeller, H.V., 2022. Thermal Responses in Global Marine Planktonic Food Webs Are Mediated by Temperature Effects on Metabolism. JGR Oceans 127, e2022JC018932. https://doi.org/10.1029/2022JC018932

Baas Becking, L., 1934. Geobiologie of inleiding tot de milieukunde. The Hague.

Bopp, L., Resplandy, L., Orr, J., Doney, S., Dunne, J., Gehlen, M., Halloran, P., Heinze, C., Ilyina, T., Séférian, R., Tjiputra, J., Vichi, M., 2013. Multiple stressors of ocean ecosystems in the 21st century: Projections with CMIP5 models. Biogeosciences 10, 6225–6245. https://doi.org/10.5194/bg-10-6225-2013

Boyd, P., Collins, S., Dupont, S., Fabricius, K., Gattuso, J., Havenhand, J., Hutchins, D., Riebesell, U., Rintoul, M., Vichi, M., Biswas, H., Ciotti, A., Gao, K., Gehlen, M., Hurd, C., Kurihara, H., McGraw, C., Navarro, J., Nilsson, G., Passow, U., Pörtner, H., 2018. Experimental strategies to assess the biological ramifications of multiple drivers of global ocean change—A review. Global Change Biology 24, 2239–2261. https://doi.org/10.1111/gcb.14102

Brennan, G., Colegrave, N., Collins, S., 2017. Evolutionary consequences of multidriver environmental change in an aquatic primary producer. Proceedings of the National Academy of Sciences of the United States of America 114, 9930–9935. https://doi.org/10.1073/pnas.1703375114

Burger, F., Terhaar, J., Frölicher, T., 2022. Compound marine heatwaves and ocean acidity extrems. Nature Communications 13, 1–12. https://doi.org/10.1038/s41467-022-32120-7

Chaffron, S., Delage, E., Budinich, M., Vintache, D., Henry, N., Nef, C., Ardyna, M., Zayed, A.A., Junger, P.C., Galand, P.E., Lovejoy, C., Murray, A.E., Sarmento, H., Tara Oceans coordinators, Acinas, S.G., Babin, M., Iudicone, D., Jaillon, O., Karsenti, E., Wincker, P., Karp-Boss, L., Sullivan, M.B., Bowler, C., de Vargas, C., Eveillard, D., 2021. Environmental vulnerability of the global ocean epipelagic plankton community interactome. Sci. Adv. 7, eabg1921. https://doi.org/10.1126/sciadv.abg1921

Chen, B., Smith, S.L., Wirtz, K.W., 2019. Effect of phytoplankton size diversity on primary productivity in the North Pacific: trait distributions under environmental variability. Ecology Letters 22, 56–66. https://doi.org/10.1111/ele.13167

Cherabier, P., Ferrière, R., 2022. Eco-evolutionary responses of the microbial loop to surface ocean warming and consequences for primary production. ISME J 16, 1130–1139. https://doi.org/10.1038/s41396-021-01166-8

Collins, S., Rost, B., Rynearson, T., 2014. Evolutionary potential of marine phytoplankton under ocean acidification. Evolutionary Applications 7, 140–155. https://doi.org/10.1111/eva.12120

Demory, D., Baudoux, A., Monier, A., Simon, N., Six, C., Ge, P., Rigaut-Jalabert, F., Marie, D., Sciandra, A., Bernard, O., Rabouille, S., 2019. Picoeukaryotes of the Micromonas genus: sentinels of a warming ocean. ISME Journal 13, 132–146. https://doi.org/10.1038/s41396-018-0248-0

DuRand, M., Olson, R., Chisholm, S., 2001. Phytoplankton population dynamics at the Bermuda Atlantic Time-series station in the Sargasso Sea. Deep-Sea Research Part II: Topical Studies in Oceanography 48, 1983–2003. https://doi.org/10.1016/S0967-0645(00)00166-1

Eppley, R., 1972. Temperature and phytoplankton growth in

the sea. Fishery Bulletin 70, 1063–1085.

Field, C., Behrenfeld, M., Randerson, J., Falkowski, P., 1998. Primary production of the biosphere: integrating terrestrial and oceanic components. Science 281, 237–240.

Flombaum, P., Gallegos, J., Gordillo, R., Zabala, L., Jiao, N., Karl, D., Li, W., Lomas, M., Veneziano, D., Vera, C., Vrugt, J., Martiny, A., 2013. Present and future global distributions of the marine Cyanobacteria Prochlorococcus and Synechococcus. Proceedings of the National Academy of Sciences of the United States of America 110, 9824–9829. https://doi.org/10.1073/pnas.1307701110/-/DCSupplemental.www.pnas.org/cgi/doi/10.1073/pnas.1307701110

Follows, M., Dutkiewicz, S., Grant, S., Chisholm, S., 2007. Emergent biogeography of microbial communities in a model ocean. Science 315, 1843–1846. https://doi.org/10.1126/science.1138544

Frölicher, T., Fischer, E., Gruber, N., 2018. Marine heatwaves under global warming. Nature 560, 360–364. https://doi.org/10.1038/s41586-018-0383-9

Grimaud, G., Le Guennec, V., Ayata, S., Mairet, F., Sciandra, A., Bernard, O., 2015. Modelling the effect of temperature on phytoplankton growth across the global ocean. IFAC-PapersOnLine 28, 228–233. https://doi.org/10.1016/j.ifacol.2015.05.059

Grimaud, G., Mairet, F., Sciandra, A., Bernard, O., 2017. Modeling the temperature effect on the specific growth rate of phytoplankton: a review. Reviews in Environmental Science and Biotechnology 16, 625–645. https://doi.org/10.1007/s11157-017-9443-0

Gruber, N., Boyd, P., Frölicher, T., Vogt, M., 2021. Ocean Biogeochemical Extremes and Compound Events. Nature 395–407. https://doi.org/10.1038/s41586-021-03981-7

Henson, S., Cael, B., Allen, S., Dutkiewicz, S., 2021. Future phytoplankton diversity in a changing climate. Nature Communications. https://doi.org/10.1038/s41467-021-25699-w

Henson, S., Sanders, R., Madsen, E., Morris, P., Le Moigne, F., Quartly, G., 2011. A reduced estimate of the strength of the ocean's biological carbon pump. Geophysical Research Letters 38, 10–14. https://doi.org/10.1029/2011GL046735

Irwin, A., Finkel, Z., Müller-Karger, F., Ghinaglia, L., 2015. Phytoplankton adapt to changing ocean environments. Proceedings of the National Academy of Sciences of the United States of America 112, 5762–5766. https://doi.org/10.1073/pnas.1414752112

Law, R., 1979. Optimal Life Histories Under Age-Specific Predation. The American naturalist 114, 399–417.

Le Gland, G., Vallina, S., Smith, S., Cermeño, P., 2021. SPEAD 1.0 – Simulating Plankton Evolution with Adaptive Dynamics in a two-trait continuous fitness landscape applied to the Sargasso Sea. Geoscientific Model Development 14, 1949–1985. https://doi.org/10.5194/gmd-14-1949-2021

Leibold, M., Norberg, J., 2004. Biodiversity in metacommunities: Plankton as complex adaptive systems? Limnology and Oceanography 49, 1278–1289. https://doi.org/10.4319/lo.2004.49.4_part_2.1278

Litchman, E., Edwards, K., Klausmeier, C., Thomas, M., 2012. Phytoplankton niches, traits and eco-evolutionary responses to global environmental change. Marine Ecology Progress Series 470, 235–248. https://doi.org/10.3354/meps09912

Loeuille, N., Leibold, M., 2008. Evolution in metacommunities: On the relative importance of species sorting and monopolization in structuring communities. American Naturalist 171, 788–799. https://doi.org/10.1086/587745

Marañón, E., Lorenzo, M.P., Cermeño, P., Mouriño-Carballido, B., 2018. Nutrient limitation suppresses the temperature dependence of phytoplankton metabolic rates. ISME J 12, 1836–1845. https://doi.org/10.1038/s41396-018-0105-1

Merico, A., Brandt, G., Smith, S., Oliver, M., 2014. Sustaining diversity in trait-based models of phytoplankton communities. Frontiers in Ecology and Evolution 2, 1–8. https://doi.org/10.3389/fevo.2014.00059

Monod, J., 1949. The growth of bacterial cultures. Annual Reviews in Microbiology.

Mouw, C.B., Ciochetto, A.B., Yoder, J.A., 2019. A Satellite Assessment of Environmental Controls of Phytoplankton Community Size Structure. Global Biogeochemical Cycles 33, 540–558. https://doi.org/10.1029/2018GB006118

Norberg, J., 2004. Biodiversity and ecosystem functioning: A complex adaptive systems approach. Limnology and Oceanography 49, 1269–1277. https://doi.org/10.4319/lo.2004.49.4_part_2.1269

O'Donnell, D.R., Du, Z., Litchman, E., 2019. Experimental evolution of phytoplankton fatty acid thermal reaction norms. Evolutionary Applications 12, 1201–1211. https://doi.org/10.1111/eva.12798

Oliver, E., Burrows, M., Donat, M., Sen Gupta, A., Alexander, L., Perkins-Kirkpatrick, S., Benthuysen, J., Hobday, A., Holbrook, N., Moore, P., Thomsen, M., Wernberg, T., Smale, D., 2019. Projected Marine Heatwaves in the 21st Century and the Potential for Ecological Impact. Frontiers in Marine Science 6, 1–12. https://doi.org/10.3389/fmars.2019.00734

Oliver, E., Donat, M., Burrows, M., Moore, P., Smale, D., Alexander, L., Benthuysen, J., Feng, M., Sen Gupta, A., Hobday, A., Holbrook, N., Perkins-Kirkpatrick, S., Scannell, H., Straub, S., Wernberg, T., 2018. Longer and more frequent marine heatwaves over the past century. Nature Communications 9, 1–12. https://doi.org/10.1038/s41467-018-03732-9

Padfield, D., Yvon-Durocher, G., Buckling, A., Jennings, S., Yvon-Durocher, G., 2016. Rapid evolution of metabolic traits explains thermal adaptation in phytoplankton. Ecology Letters 19, 133–142. https://doi.org/10.1111/ele.12545

Saba, V., Friedrichs, M., Carr, M., Antoine, D., Armstrong, R., Asanuma, I., Aumont, O., Bates, N., Behrenfeld, M., Bennington, V., Bopp, L., Bruggeman, J., Buitenhuis, E., Church, M., Ciotti, A., Doney, S., Dowell, M., Dunne, J., Dutkiewicz, S., Gregg, W., Hoepffner, N., Hyde, K., Ishizaka, J., Kameda, T., Karl, D., Lima, I., Lomas, M., Marra, J., McKinley, G., Melin, F., Moore, J., Morel, A., O'Reilly, J., Salihoglu, B., Scardi, M., Smyth, T., Tang, S.,

Tjiputra, J., Uitz, J., Vichi, M., Waters, K., Westberry, T., Yool, A., 2010. Challenges of modeling depth-integrated marine primary productivity over multiple decades: A case study at BATS and HOT. Global Biogeochemical Cycles 24, 1–21. https://doi.org/10.1029/2009GB003655

Sallée, J.-B., Pellichero, V., Akhoudas, C., Pauthenet, E., Vignes, L., Schmidtko, S., Garabato, A.N., Sutherland, P., Kuusela, M., 2021. Summertime increases in upper-ocean stratification and mixed-layer depth. Nature 591, 592–598. https://doi.org/10.1038/s41586-021-03303-x

Sauterey, B., Ward, B., Rault, J., Bowler, C., Claessen, D., 2017. The Implications of Eco-Evolutionary Processes for the Emergence of Marine Plankton Community Biogeography. The American Naturalist 190. https://doi.org/10.1086/692067

Savage, V.M., Webb, C.T., Norberg, J., 2007. A general multi-trait-based framework for studying the effects of biodiversity on ecosystem functioning. Journal of Theoretical Biology 247, 213–229. https://doi.org/10.1016/j.jtbi.2007.03.007

Smith, S.L., Vallina, S.M., Merico, A., 2016. Phytoplankton size-diversity mediates an emergent trade-off in ecosystem functioning for rare versus frequent disturbances. Sci Rep 6, 34170. https://doi.org/10.1038/srep34170

Sunagawa, S, Acinas, S., Bork, P., Bowler, C., Babin, M., Boss, E., Cochrane, G., de Vargas, C., Follows, M., Gorsky, G., Grimsley, N., Guidi, L., Hingamp, P., Iudicone, D., Jaillon, O., Kandels, S., Karp-Boss, L., Karsenti, E., Lescot, M., Not, F., Ogata, H., Pesant, Stéphane, Poulton, N., Raes, J., Sardet, C., Sieracki, M., Speich, S., Stemmann, L., Sullivan, M.B., Sunagawa, Shinichi, Wincker, P., Eveillard, D., Gorsky, G., Guidi, L., Iudicone, D., Karsenti, E., Lombard, F., Ogata, H., Pesant, Stephane, Sullivan, M.B., Wincker, P., de Vargas, C., 2020. Tara Oceans: towards global ocean ecosystems biology. Nat Rev Microbiol 18, 428–445. https://doi.org/10.1038/s41579-020-0364-5

Thomas, M., Kremer, C., Klausmeier, C., Litchman, E., 2012. A global pattern of thermal adaptation in marine phytoplankton. Science 338, 1085–1088. https://doi.org/10.1126/science.1224836

Vallina, S.M., Cermeno, P., Dutkiewicz, S., Loreau, M., Montoya, J.M., 2017. Phytoplankton functional diversity increases ecosystem productivity and stability. Ecological Modelling 361, 184–196. https://doi.org/10.1016/j.ecolmodel.2017.06.020

Ward, B.A., Cael, B.B., Collins, S., Young, C., 2021. Selective constraints on global plankton dispersal. Proceedings of the National Academy of Sciences 1–7. https://doi.org/10.1073/pnas.2007388118/-/DCSupplemental.y

Ward, B.A., Collins, S., Dutkiewicz, S., Gibbs, S., Bown, P., Ridgwell, A., Sauterey, B., Wilson, J., Oschlies, A., 2019. Considering the Role of Adaptive Evolution in Models of the Ocean and Climate System. Journal of Advances in Modeling Earth Systems. https://doi.org/10.1029/2018MS001452

Ward, B.A., Marañón, E., Sauterey, B., Rault, J., Claessen, D., 2017. The Size Dependence of Phytoplankton Growth Rates: A Trade-Off between Nutrient Uptake and Metabolism. The American Naturalist 189, 170–177. https://doi.org/10.1086/689992

Acknowledgement

This research is part of the GOMMA project founded by the CSIC – IEO (grant number PID2020-119803GB-I00).

Competing interest statement

The authors declare that they have no competing interests

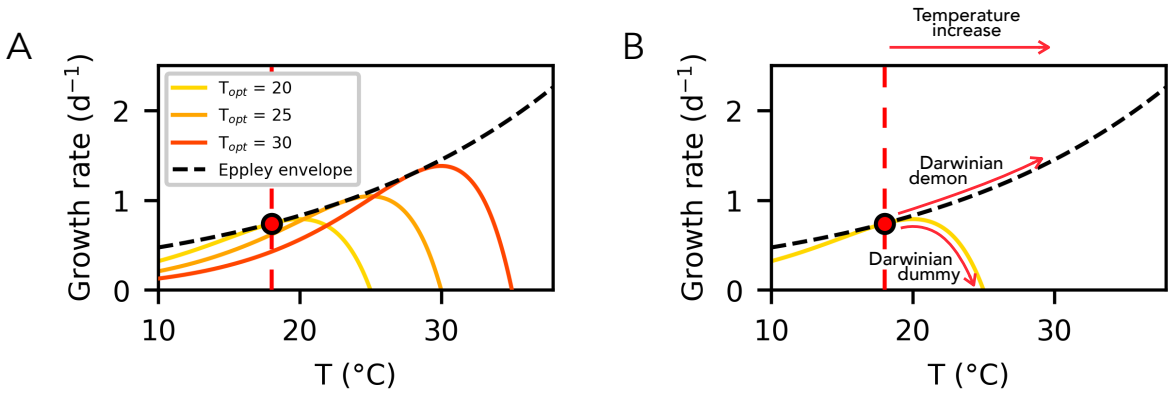

Fig. 1: Phytoplankton response to temperature changes. Panel A shows the observed relationship between the growth of phytoplankton individuals and temperature given the thermal niche of those individuals. Each colored thermal reaction norms corresponds to the thermal niche of a specific type of individuals, each niche being characterized by a temperature of optimal growth (T_{opt}). Panel B shows the expected physiological and evolutionary response of phytoplankton communities to a temperature change.

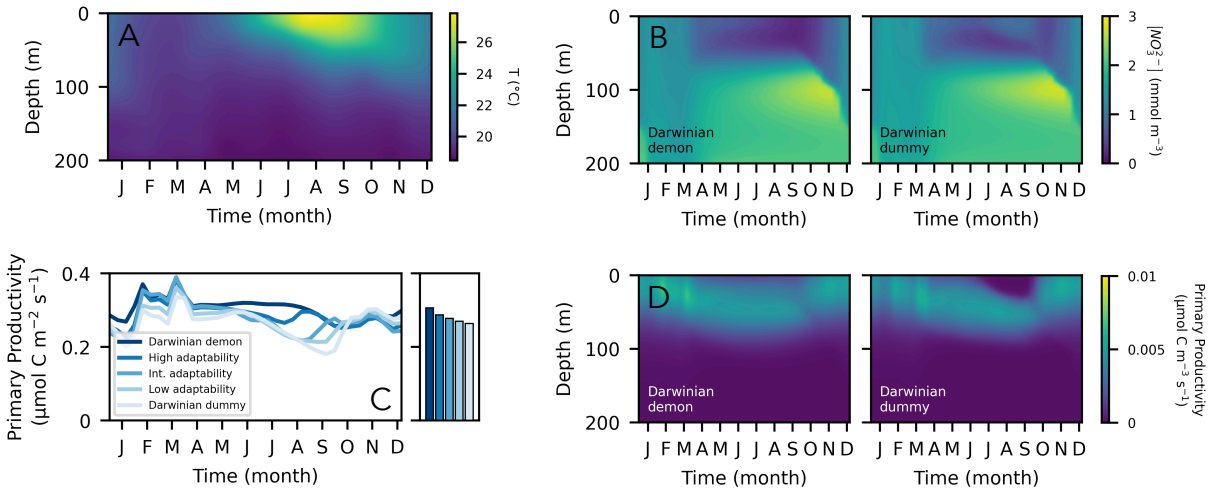

Fig. 2: Simulated ecosystem dynamics in the Bermuda-like temperate oligotrophic system. The figure shows the seasonal variation of the vertical profile of the temperature (in °C) (A**)** and of the availability of nitrate (in µmol NO_3^{2-} m^{-3}) (B), and the seasonal variation of the primary productivity (PP) of the phytoplankton (in µmol C m^{-3} s^{-1}) (C and D**)**. The colored curves in panel C correspond to the vertical integration of the predicted PP in five evolutionary scenarios: Darwinian demon, high, intermediate, low mutation rate of the phytoplankton and Darwinian Dummy. The annual means are shown as colorbars on the right hand subpanel. In panels B and D, only the predictions obtained in the two extreme scenarios (i.e., the Darwinian Demon and Dummy scenarios) are shown.

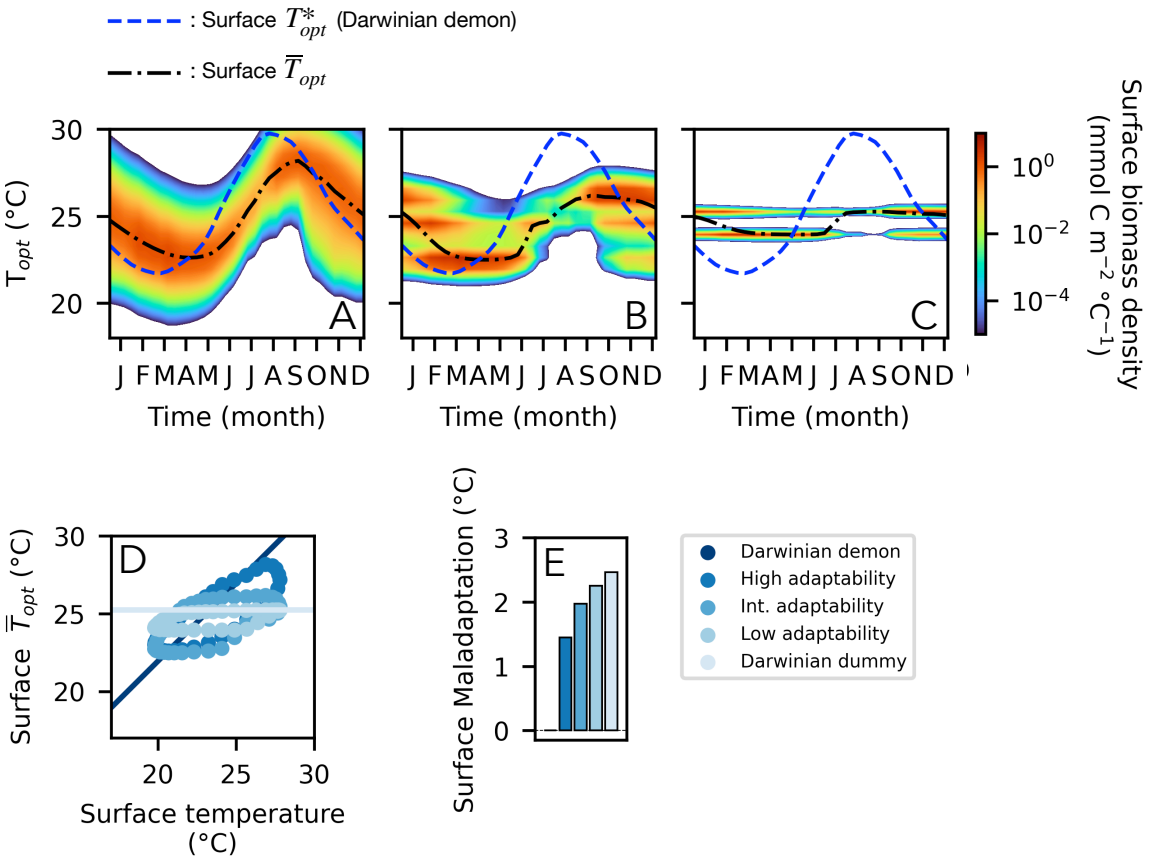

Fig. 3: Adaptive response of the phytoplankton to the seasonal change in temperature at the surface. Panels A-C show the seasonal change in the trait distribution of the phytoplankton community in the first meters of the water-column when phytoplankton mutation rate is high, intermediate and low. The black dashed line corresponds to the community average thermal niche at the surface, $\bar{T}_{opt}(0)$, and the blue dash-dotted line to the evolutionary optimal trait $T^*_{opt}(0)$ (i.e., corresponding to the trait of the perfectly adapting Darwinian demon; see Methods). Panel D shows, the match throughout the year between the average trait of the phytoplankton community at the surface $\bar{T}_{opt}(0)$ and the optimal trait $T^*_{opt}(0)$ of the Darwinian demon given surface temperatures $T(0)$ when the phytoplankton has a high, intermediate, and low mutation rate, and when the phytoplankton is a Darwinian dummy (no adaptation). For each of these evolutionary scenarios, the panel E shows the surface thermal maladaptation of the phytoplankton (measured as $M(0) = \left|\bar{T}_{opt}(0) - T^*_{opt}(0)\right|$) averaged over the year.

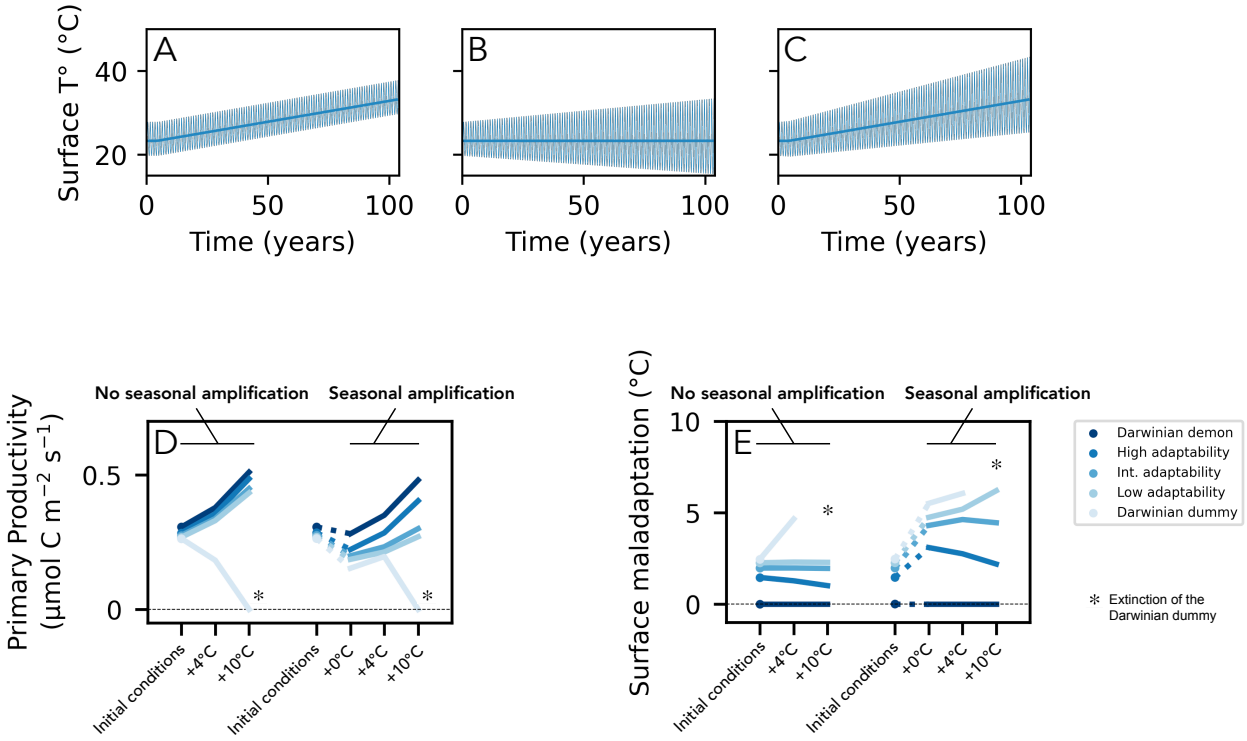

Fig. 4: Simulated regimes of temperature change over 100 years (A-C) and phytoplankton primary productivity (D) and surface maladaptation (E) before and after these changes take place depending on the adaptive capacity of the phytoplankton. Climate change is here simulated either as an increase of the average temperatures of up to 10°C (A), as +10°C increase in the amplitude of the seasonal temperature variation (B) or as both simultaneously (C). Panels D and E show the primary productivity and surface maladaptation of the phytoplankton community in the initial conditions of the system and after a global temperature increase of +4 and +10°C coupled or not to an increase in seasonal amplitude. The * signs in panels D and E indicate when there has been an extinction of the phytoplankton population in the Darwinian dummy scenario.

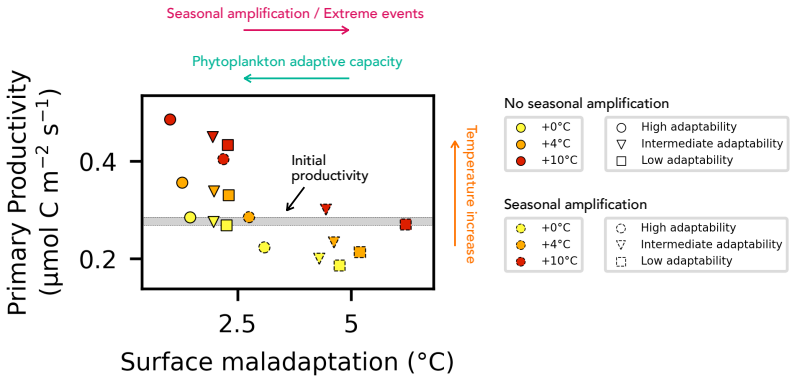

Fig. 5: Link between primary productivity, temperature increase and maladaptation of the phytoplankton. Each dot corresponds to the state of the system after 100 years of a temperature increase of +0, +4 and +10°C coupled or not with seasonal amplification. The shape of the dots corresponds to the adaptive capacity of the phytoplankton and their color to the amplitude of the temperature increase over 100 years. Dots corresponding to scenarios of seasonal amplification have dashed edges, those that do not have plain edges. We plotted only the scenarios in which the adaptive capacity of the phytoplankton is high, intermediate and low and excluded the Darwinian demon and dummy scenarios. The arrows correspond to the direction of main effect of seasonal amplification, phytoplankton adaptive capacity, and average temperature increase (in magenta, turquoise and orange respectively) on PP either directly (temperature increase) or indirectly through their effect on maladaptation (seasonal amplification and phytoplankton adaptive capacity).

Supplementary materials for

"Phytoplankton adaptive resilience to climate change collapses in case of extreme events – A modeling study"

I. Thermal niche of the phytoplankton

I.1. Parametrization

Phytoplankton growth g is described in the model as follows

$$g = g_{max} \cdot \gamma_T \cdot \gamma_N \cdot \gamma_I \cdot \gamma_{p_{CO_2}} \cdot \gamma_P \quad \text{(E1)}$$

where g_{max} is the maximum growth rate of phytoplankton individuals and γ_T, γ_N, γ_I, $\gamma_{p_{CO_2}}$ and γ_P the growth limitation factors associated with temperature, with the availability of nutrients, light, and dissolved CO_2, and with the Allee effect (see discussion below), respectively. The term γ_T corresponds to the thermal reaction norm of phytoplankton individuals (Fig. 1 and S1A). Following Le Gland et al. (2021) the thermal reaction norm $\gamma_{T,i}$ of a phytoplankton population P_i, with a temperature of optimal growth $T_{opt,i}$ is expressed as:

$$\text{(E2)} \quad \begin{aligned} &\gamma_{T,i} = e^{\alpha\left(T_{opt,i} - T_{ref}\right)} \cdot e^{\frac{T - T_{opt,i}}{\omega}} \cdot \frac{\left(T_{opt,i} + \omega - T\right)}{\omega} \text{ when } T - T_{opt,i} < \omega, \\ &\gamma_{T,i} = 0 \text{ when } T - T_{opt,i} > \omega. \end{aligned}$$

Each term corresponds to one specific aspect of the temperature dependence of phytoplankton growth (Fig. S1A). The first term describes how the maximum growth of the population i, achieved when $T = T_{opt,i}$, increases with the value of $T_{opt,i}$, following the Norberg-Eppley model, with α and T_{ref} being the exponent and reference temperature of the Eppley envelope (Le Gland et al., 2021). The second term describes how growth progressively converges toward 0 when temperatures get lower than T_{opt}. The third term describes how growth abruptly drops to zero when temperatures get higher than T_{opt}. In those two terms, ω corresponds to the thermal tolerance of the phytoplankton population. It determines how fast phytoplankton growth converges toward zero at low temperatures, and what is the higher temperature limit for which growth is superior to zero. In our simulations, we used parameter values (see supplementary table 1) in agreement with the most up to date empirical estimations (Anderson et al., 2021).

I.2. Evolutionary optimal thermal trait

For any given temperature T of the system, there is a trait T_{opt}^* that maximizes phytoplankton growth (Fig. S1B). T_{opt}^* is therefore an evolutionary optimum. By definition, the trait of the Darwinian demon is always equal to T_{opt}^*. Also by definition, when $T_{opt} = T_{opt}^*$ then $\frac{d\gamma_T(T)}{dT_{opt}} = 0$. From (E2) we get the expression of $\frac{d\gamma_T(T)}{dT_{opt}}$:

$$\text{(E3)} \quad \frac{d\gamma_T(T)}{dT_{opt}} = \frac{\left(T - T_{opt} + \alpha\omega\left(T_{opt} - T + \omega\right)\right) e^{\frac{T - T_{opt} + \alpha\omega\left(T_{opt} - T_{ref}\right)}{\omega}}}{\omega^2}.$$

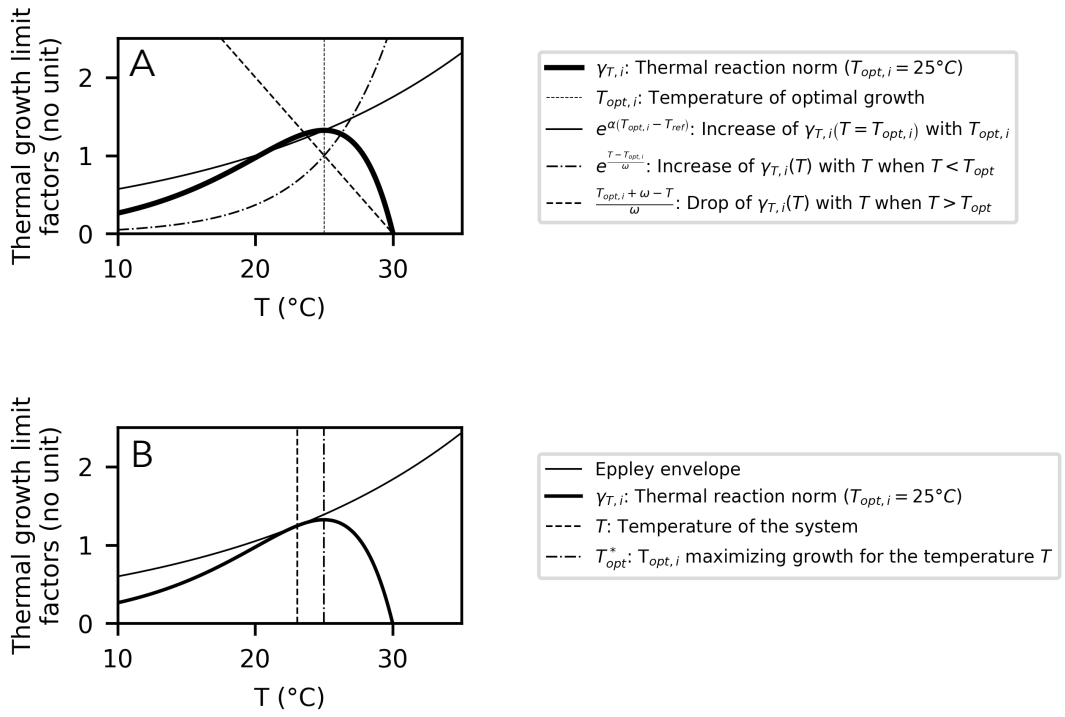

Supplementary Figure 1: Temperature dependence of phytoplankton growth. Panel A shows how the combination of three temperature dependent terms determines the shape of the thermal reaction norm of a phytoplankton population P_i characterized by a $T_{opt,i}$ = 25°C. Panel B shows how, for a given temperature T, growth is maximized by a phytoplankton population characterized by a $T_{opt} = T^*_{opt} \approx T + 1.94$°C.

Solving $\frac{d\gamma_T(T)}{dT_{opt}} = 0$ is therefore equivalent to solving $\left(T - T_{opt} + \alpha\omega\left(T_{opt} - T + \omega\right)\right) = 0$. This equation accepts the solution

$$T^*_{opt} = T + \frac{\alpha\omega^2}{1-\alpha\omega}. \quad \text{(E4)}$$

With the parametrization used in our simulation, $T^*_{opt} \approx T + 1.94$ °C.

Supplementary Table 1: temperature dependence of phytoplankton growth

Parameter	symbol	value	unit
Eppley exponent	α	0.056	°C^{-1}
Eppley reference temperature	T_{ref}	20	°C
Thermal tolerance	ω	5	°C

II. Eco-evolutionary model

II.1. Discrete trait-diffusion method

The model solves the population dynamics of 50 phytoplankton “subtypes”. Each of these subtypes P_i is characterized by a specific thermal niche and by a specific temperature of optimal growth $T_{opt,i}$, ranging

from 18°C to 50.34°C by increment of 0.66°C. We refer to the ensemble of these populations as the phytoplankton community, and to the relative abundance of those subtypes as the functional composition of the phytoplankton community. The net growth rate of these phytoplankton populations is expressed as:

$$(E5) \quad s_i = (g_i - d)P_i$$

where g_i, the individual growth rate of the population P_i, depends on the adequation of the trait of the population $T_{opt,i}$ and the temperature of the system T according to equations (E1) and (E2) and where d is mortality. This net growth rate corresponds to the fitness of each of the 50 populations. Additionally, the model describes how, at each generation, a proportion of the offspring produced by each population is carrying phenotypically altering mutations that results in their trait being different from that of their ancestors. The effect of this mutational process on the functional composition of the phytoplankton community is simulated as a diffusion process (Le Gland et al., 2021; Leimar et al., 2008; Merico et al., 2014; Sauterey et al., 2017; Smith et al., 2016; Van Der Laan and Hogeweg, 1995) as follows:

$$(E6) \quad \frac{dP_i}{dt} = s_i + \nu \cdot \sigma^2 \frac{\partial^2 g_i P_i}{\partial {T_{opt}}^2}$$

where ν is the probability of a mutation occurring (i.e., the mutation rate) at each division event, σ the average phenotypic effect of this mutation (here considered to be equal to one), and $\frac{\partial^2 g_i P_i}{\partial {T_{opt}}^2}$ the local gradient (around $T_{opt,i}$) of the individual division rate along the dimension of the trait T_{opt}. The second term of this expression therefore describes the mutational flux of individuals in and out of the population P_i. By considering 50 phytoplankton subtypes – hence a finite number of 50 trait values – instead of considering the fate of individuals carrying every possible values of T_{opt}, we actually perform a discrete approximation of the trait space. In the context of this approximation, the equation (E6) becomes

$$(E7) \quad \begin{aligned} &\frac{dP_i}{dt} = s_i + \nu \cdot \sigma^2 \frac{g_{i+1}P_{i+1} + g_{i-1}P_{i-1} - 2g_iP_i}{\Delta {T_{opt}}^2}, \\ &\frac{dP_i}{dt} = s_i + \nu \cdot \sigma^2 \frac{g_{i+1}P_{i+1} - g_iP_i}{\Delta {T_{opt}}^2} \text{ when i = 0 and} \\ &\frac{dP_i}{dt} = s_i + \nu \cdot \sigma^2 \frac{g_{i-1}P_{i-1} - g_iP_i}{\Delta {T_{opt}}^2} \text{ when i = 50.} \end{aligned}$$

with $\Delta T_{opt} = 0.66$°C. The range of thermal optima corresponding to the phytoplankton community is very large and includes unrealistically high values. We have voluntarily set low and high limits to the T_{opt} range considered to avoid boundary effects when assuming high mutation rates (i.e., tails of the trait distributions being cut off when reaching those boundary trait values). This is particularly necessary toward the higher end of the T_{opt} range as trait distributions tend to be skewed in that direction because of the asymmetry of the thermal reaction norm.

II.2. Allee effect

One of the known drawbacks of that method of simulating eco-evolutionary process (Perthame and Gauduchon, 2009; Sauterey et al., 2017) is that the diffusion terms tend to result in the emergence of trait distributions characterized by infinitely long tails of infinitesimal populations because continuous model of population cannot by design reproduce extinction (populations converge toward an abundance of zero without ever actually reaching it). Although it is not a problem when considering a biological system under continuous selective pressure, it can become one when considering a fluctuating ecosystem such as a seasonal oceanic ecosystem. Those infinitesimally rare populations can then take over the ecosystem

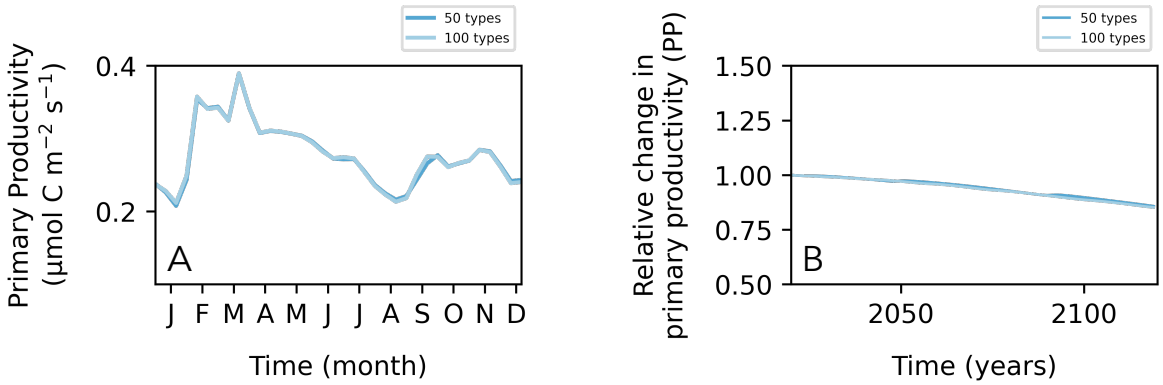

Supplementary Figure 2: Model sensitivity to the number of included types. Panel **A** and **B** respectively show the primary productivity of the ecosystem and its evolution under a regime of climate change of +4°C and +10°C of seasonal amplitude over 100 years assuming an intermediate adaptive capacity of the phytoplankton (υ = 10^{-5}) when including 50 and 100 subtypes in the model (darker and lighter blue respectively).

after a brusque change in the environmental conditions favorable to them, thus generating unrealistic evolutionary jumps. Following Perthame and Gauduchon (2009), to solve this problem, we implement to our model of phytoplankton growth an Allee effect γ_P (from the seminal work of Allee et al. 1949) which describes how the fitness of the individuals of the population P_i drops with the population abundance:

$$\text{(E8)} \quad \gamma_P = \frac{P_i}{P_i + A}$$

where A is the Allee constant such that when $P_i = A$ the individuals' growth rate is half of their maximal growth rate. This limiting factor results in the population growth rapidly dropping toward 0 when $P_i << A$. We set the value of A at 10^{-8} mmol C m^{-3} so that it would only affect very rare ecotypes. Consequently, those rare ecotypes can take over the ecosystem after an environmental change only if it has been reintroduced in the system at sufficient levels of abundance, either by mutation, or by vertical mixing.

II.3. Sensitivity to the number of ecotypes included in the model

Discrete resolution of trait-diffusion is known to be sensitive to the number of subtypes included in the model. When this number becomes too low, the speed of the evolutionary process tends to be overestimated (supplementary materials of Sauterey et al. (2017). In order to assess whether it was the case in our 50-types configuration, we ran simulations with 100 types distributed along the same range of thermal optima (18 to 50.34°C) resolving the initial state of the ecosystem and its response to an intermediate increase in average temperature of 4°C over 100 years coupled to a seasonal amplification while assuming an intermediate mutation rate of 10^{-5}. We obtain almost exactly the same results when including 50 and 100 phytoplankton types (Supplementary Figure 2).

III. <u>Interacting effects of nutrient availability and temperature change on thermal adaptation</u>

In the context of climate change, phytoplankton populations are expected to face multiple environmental stresses in addition to long-term and short-term temperature changes. It remains unclear how the combination of these multiple environmental stresses will affect the physiological and adaptive responses of phytoplankton individuals and communities to every individual stress (Boyd et al., 2018; Brennan et al., 2017; Marañón et al., 2018). As mentioned in the core of this study, we artificially isolated the effect of temperature on phytoplankton from any other environmental stresses. Would our predictions change should other environmental stresses be accounted for? In a first attempts at answering this question, we ran new sets of simulations in which, in addition to an average temperature increase of 4°C and an

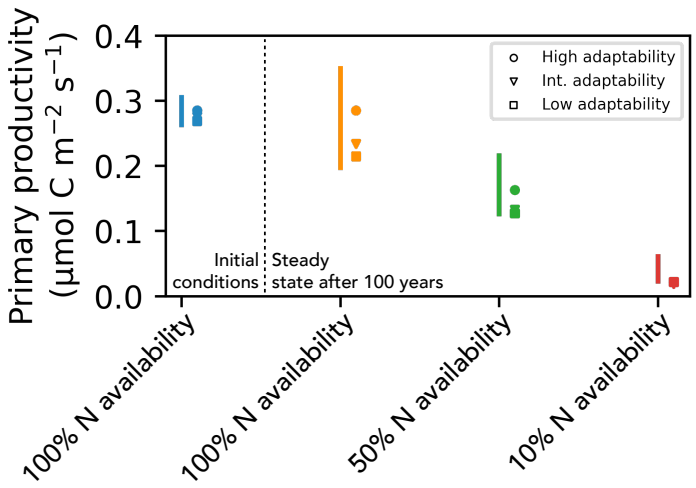

Supplementary Figure 3: Ranges of predicted surface primary productivity as a function of nitrogen (N) availability in the water column. The blue, orange, green and red vertical lines correspond to the ranges of predicted primary productivity prior to climate change and after 100 years of climate change without reduction of the nutrient availability, with nutrient availability being reduced by a factor 2, or by a factor 10, respectively. The climate change consists of +4°C increase in average temperature and a +10°C increase in temperature annual variability. The minimum value of the range corresponds to the Darwinian dummy scenario, the maximum value to the Darwinian demon scenario. The circles, triangles and squares correspond to the scenarios of high, intermediate, and low adaptive capacity of the phytoplankton respectively.

increase in seasonal variation of temperature of 10°C, the phytoplankton is also exposed to a reduction of the nutrient availability by a factor 2 and 10. Contrary to the regime of temperature change, this reduction of the nutrient availability takes place at the beginning of the simulation, not progressively throughout the 100 years of the simulation. The results are shown in Figure S3.

First, we find that a decrease in nutrient availability can counteract the effect of temperature increase on phytoplankton growth and can break down the prediction of increased primary productivity in a regime of climate change. Second, we find that although the relative spread of the prediction range remains of the same order regardless of nutrient availability (i.e., the minimum predicted value of primary productivity is lower than the maximum by 43, 41 and 62% when nutrient availability is unchanged, divided by 2 and divided by 10, respectively), the absolute spread of the predictions drops as nutrient availability is decreased. Finally, we find that the adaptive capacity of the phytoplankton increasingly diverges from the Darwinian demon scenario as the nutrient availabilities considered are smaller: nutrient depleted conditions result to lower division rates which in turn results in a decreased rate of adaptation by the phytoplankton. We see this last result as particularly interesting as it highlights that adaptation of specific functional traits (here the thermal niche) might be influenced by apparently unrelated environmental stressors (here nutrient availability) and suggests that studying such interacting effects in the more realistic context of a 3D circulation model might be key to better predict the overall adaptive response of phytoplankton communities to multi-faceted environmental changes.

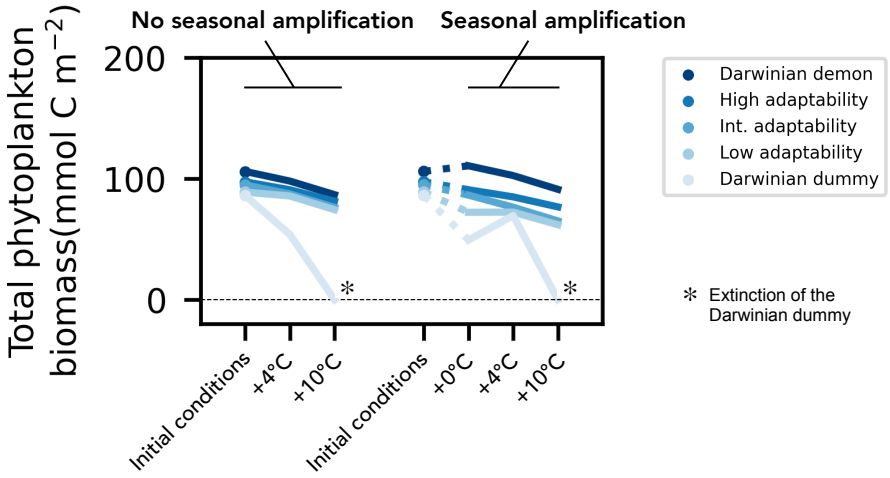

Supplementary Figure 4: Total depth integrated phytoplankton biomass before and after temperature changes operating over 100 years, and depending on the adaptive capacity of the phytoplankton. The different shades of blue correspond to the different evolutionary scenarios. The * sign indicates events of complete extinction of the phytoplankton populations in the Darwinian dummy scenario.

Supplementary references

1. Anderson, S., Barton, A., Clayton, S., Dutkiewicz, S., Rynearson, T., 2021. Marine phytoplankton functional types exhibit diverse responses to thermal change. Nature Communications 12, 1–9. https://doi.org/10.1038/s41467-021-26651-8

2. Boyd, P., Collins, S., Dupont, S., Fabricius, K., Gattuso, J., Havenhand, J., Hutchins, D., Riebesell, U., Rintoul, M., Vichi, M., Biswas, H., Ciotti, A., Gao, K., Gehlen, M., Hurd, C., Kurihara, H., McGraw, C., Navarro, J., Nilsson, G., Passow, U., Pörtner, H., 2018. Experimental strategies to assess the biological ramifications of multiple drivers of global ocean change—A review. Global Change Biology 24, 2239–2261. https://doi.org/10.1111/gcb.14102

3. Brennan, G., Colegrave, N., Collins, S., 2017. Evolutionary consequences of multidriver environmental change in an aquatic primary producer. Proceedings of the National Academy of Sciences of the United States of America 114, 9930–9935. https://doi.org/10.1073/pnas.1703375114

4. Le Gland, G., Vallina, S., Smith, S., Cermeño, P., 2021. SPEAD 1.0 – Simulating Plankton Evolution with Adaptive Dynamics in a two-trait continuous fitness landscape applied to the Sargasso Sea. Geoscientific Model Development 14, 1949–1985. https://doi.org/10.5194/gmd-14-1949-2021

5. Leimar, O., Doebeli, M., Dieckmann, U., 2008. Evolution of phenotypic clusters through competition and local adaptation along an environmental gradient. Evolution 62, 807–822.

6. Marañón, E., Lorenzo, M.P., Cermeño, P., Mouriño-Carballido, B., 2018. Nutrient limitation suppresses the temperature dependence of phytoplankton metabolic rates. ISME J 12, 1836–1845. https://doi.org/10.1038/s41396-018-0105-1

7. Merico, A., Brandt, G., Smith, S., Oliver, M., 2014. Sustaining diversity in trait-based models of phytoplankton communities. Frontiers in Ecology and Evolution 2, 1–8.

https://doi.org/10.3389/fevo.2014.00059

8. Perthame, B., Gauduchon, M., 2009. Survival thresholds and mortality rates in adaptive dynamics: conciliating deterministic and stochastic simulations. Mathematical Medicine and Biology 27, 195–210. https://doi.org/10.1093/imammb/dqp018

9. Sauterey, B., Ward, B., Rault, J., Bowler, C., Claessen, D., 2017. The Implications of Eco-Evolutionary Processes for the Emergence of Marine Plankton Community Biogeography. The American Naturalist 190. https://doi.org/10.1086/692067

10. Smith, S.L., Vallina, S.M., Merico, A., 2016. Phytoplankton size-diversity mediates an emergent trade-off in ecosystem functioning for rare versus frequent disturbances. Sci Rep 6, 34170. https://doi.org/10.1038/srep34170

11. Van Der Laan, J., Hogeweg, P., 1995. Predator-prey coevolution: interactions across different timescales. Proceedings of the Royal Society, London 259, 35–42.